Electronic Supplementary Material (ESI) for Reaction Chemistry & Engineering.

Electronic Supplementary Information

Roles of ethanol and Si-OH in aldol condensation of ethyl acetate over a Cs/SBA-15 catalyst

Xiang Tian and Hengshui Tian*

College of Chemical Engineering, East China University of Science and Technology, Shanghai 200237, People's Republic of China

*Corresponding author:

Prof. Hengshui Tian

130 Meilong Road Xuhui District Shanghai city

200237 P. R. China

Tel.: +86 21 64252198

E-Mail: hengshuitian@126.com

This file includes fifteen figures and four tables:

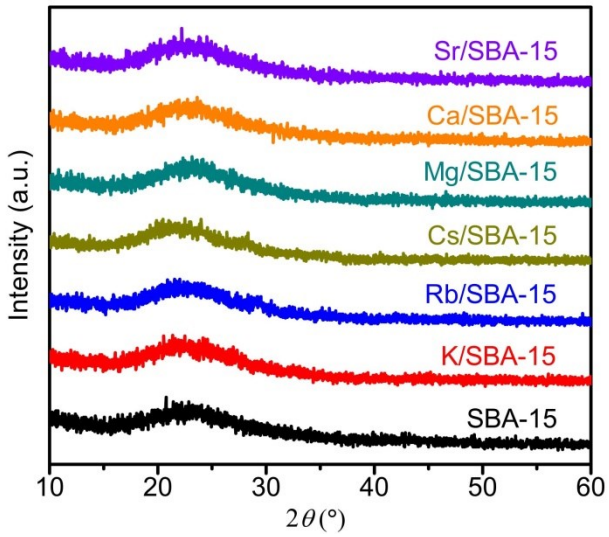

Fig. S1. Wide-angle XRD patterns of the screened catalysts.

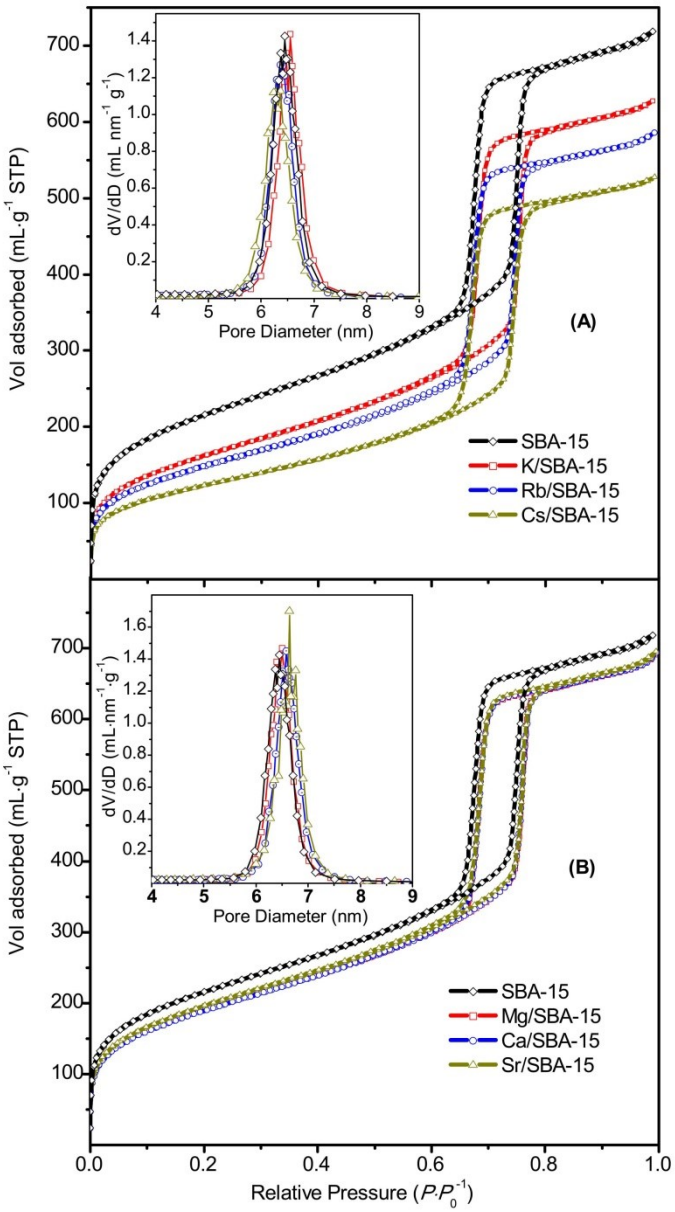

Fig. S2. N_2 adsorption-desorption isotherms and pore size distributions of the screened catalysts: (A) alkali metal and (B) alkaline earth metal.

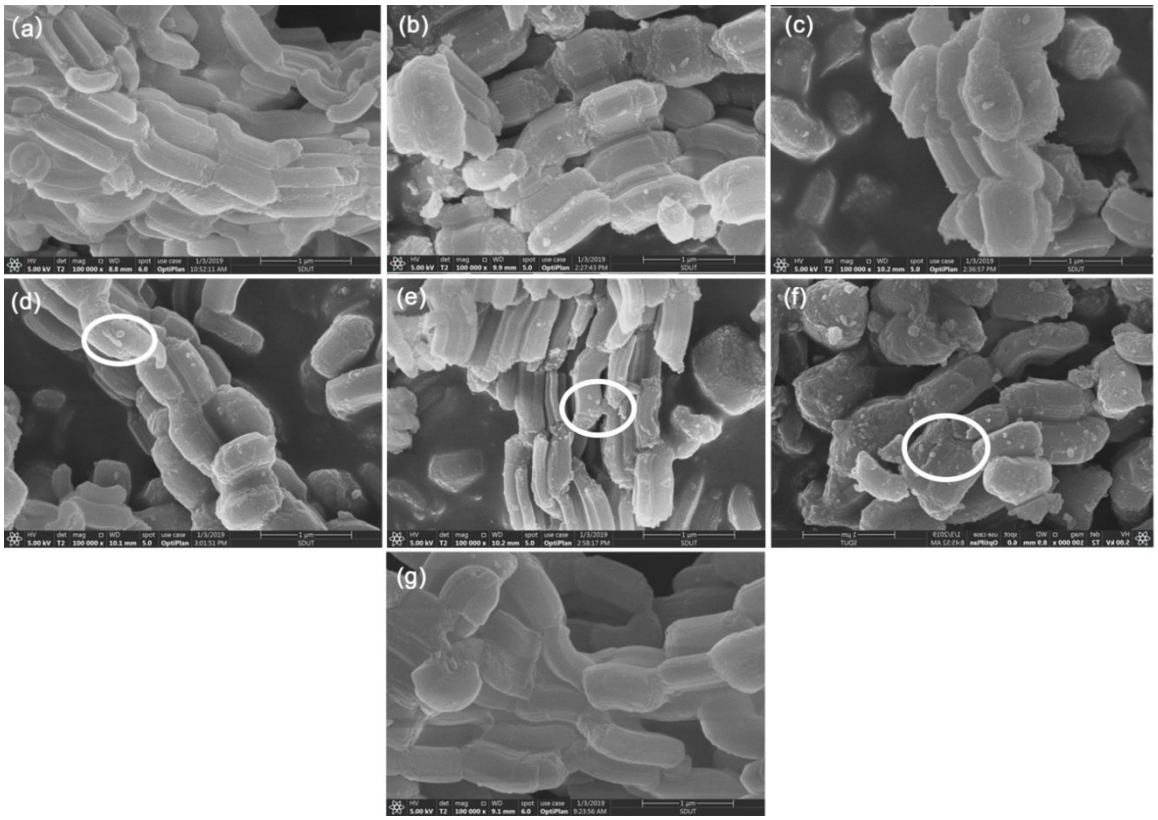

Fig. S3. SEM images of the screened catalysts: (a) Mg/SBA-15, (b) Ca/SBA-15, (c) Sr/SBA-15, (d) K/SBA-15, (e) Rb/SBA-15, (f) Cs/SBA-15 and (g) SBA-15.

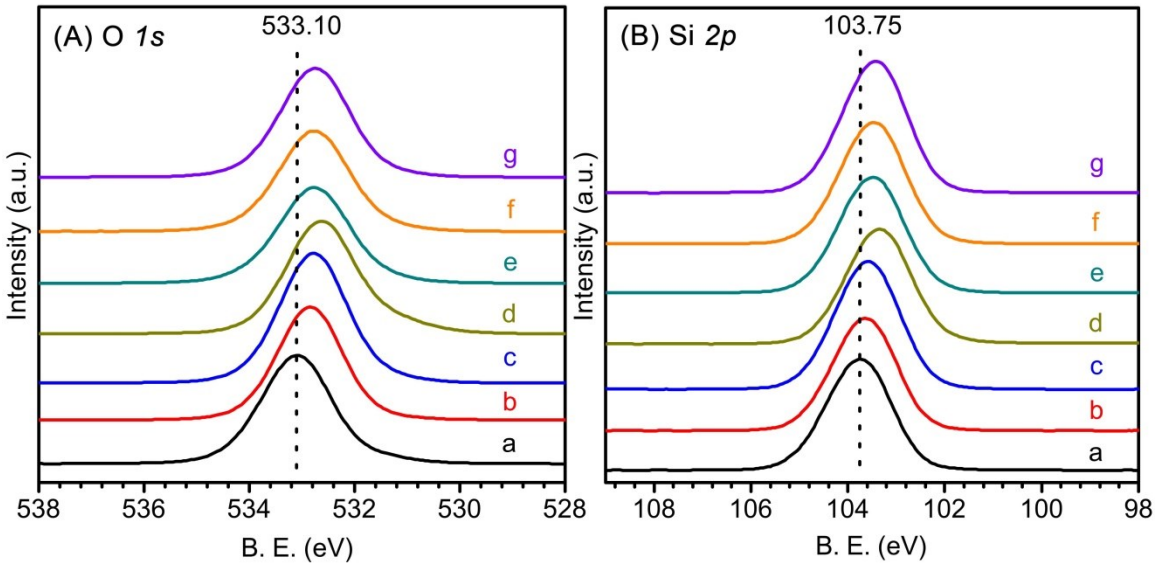

Fig. S4. X-ray photoelectron spectra of the (A) O *1s* and (B) Si *2p* region: (a) SBA-15, (b) K/SBA-15, (c) Rb/SBA-15, (d) Cs/SBA-15, (e) Mg/SBA-15, (f) Ca/SBA-15, and (g) Sr/SBA-15.

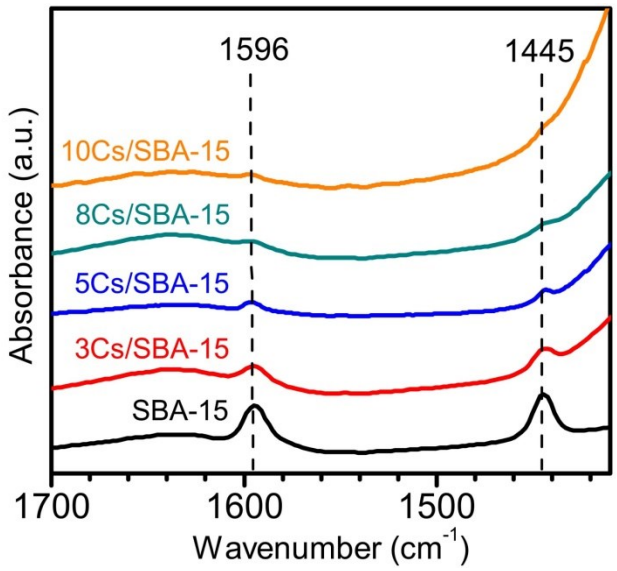

Fig. S5. Pyridine-FTIR spectra for xCs/SBA-15 catalyst.

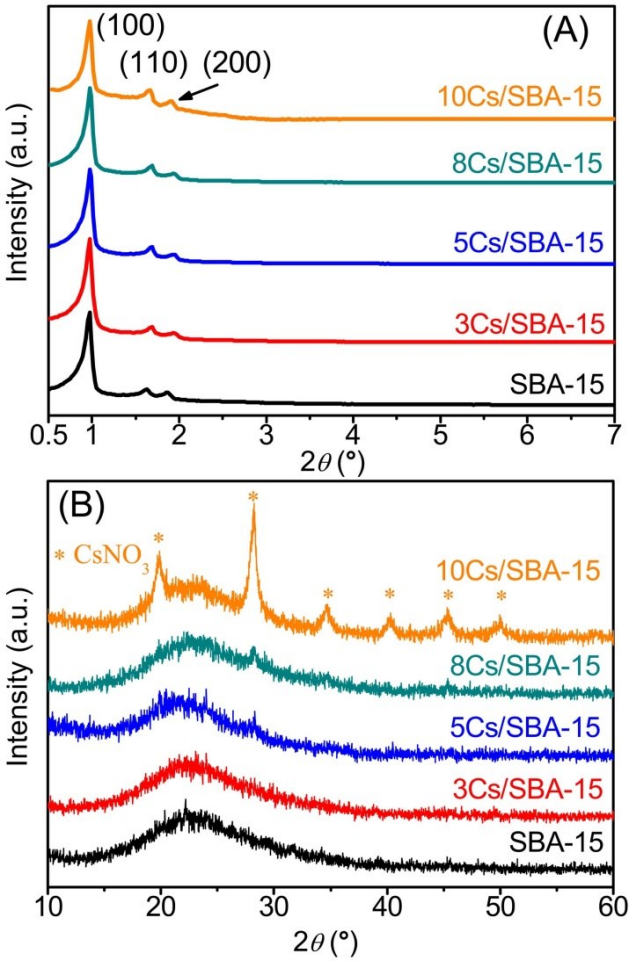

Fig. S6. XRD patterns of SBA-15 and the Cs/SBA-15 with different loading: (A) small-angle and (B) wide-angle.

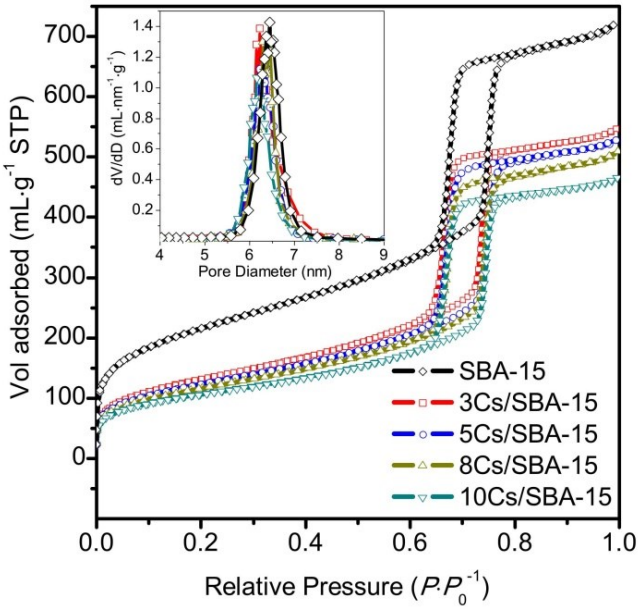

Fig. S7. N2 adsorption-desorption isotherms and pore size distributions of SBA-15 and xCs/SBA-15 catalyst.

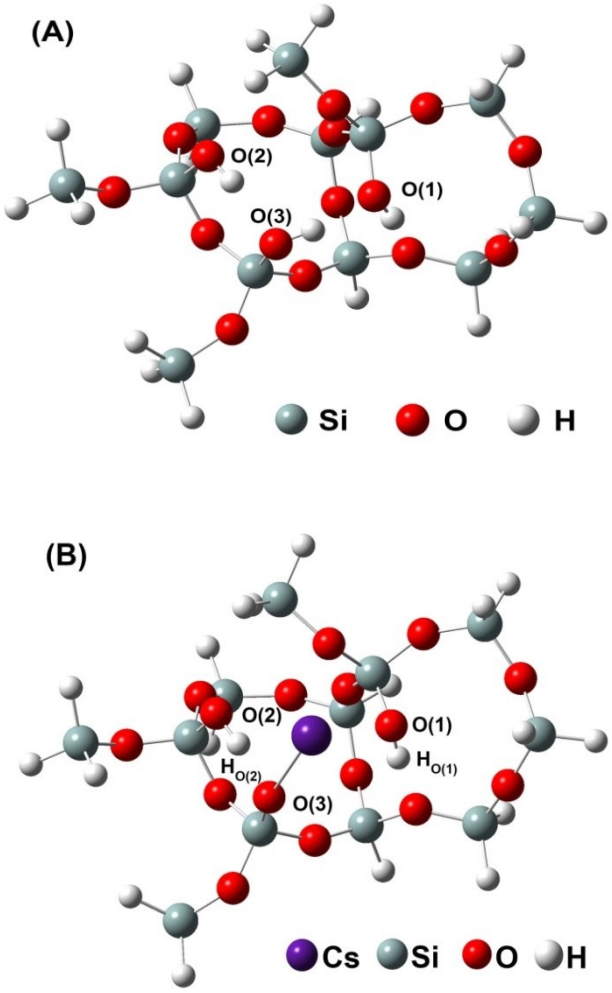

Fig. S8. The depictures of (A) model of SBA-15 and (B) model of Cs/SBA-15.

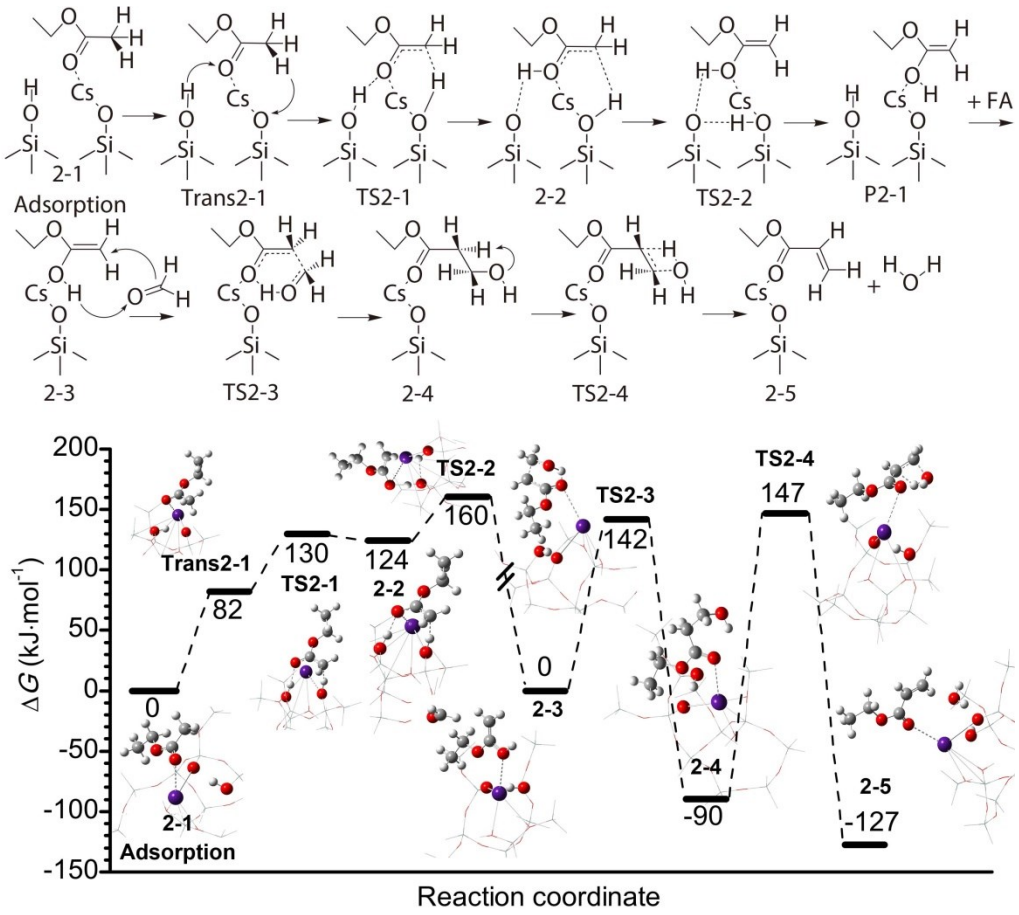

Fig. S9. The scheme and the total energy diagram for the pathway of aldol condensation between Ea and FA through the route of enol structure on the active surface model of Cs/SBA-15. Two parallel bars indicate that the contribution of FA starts to be included.

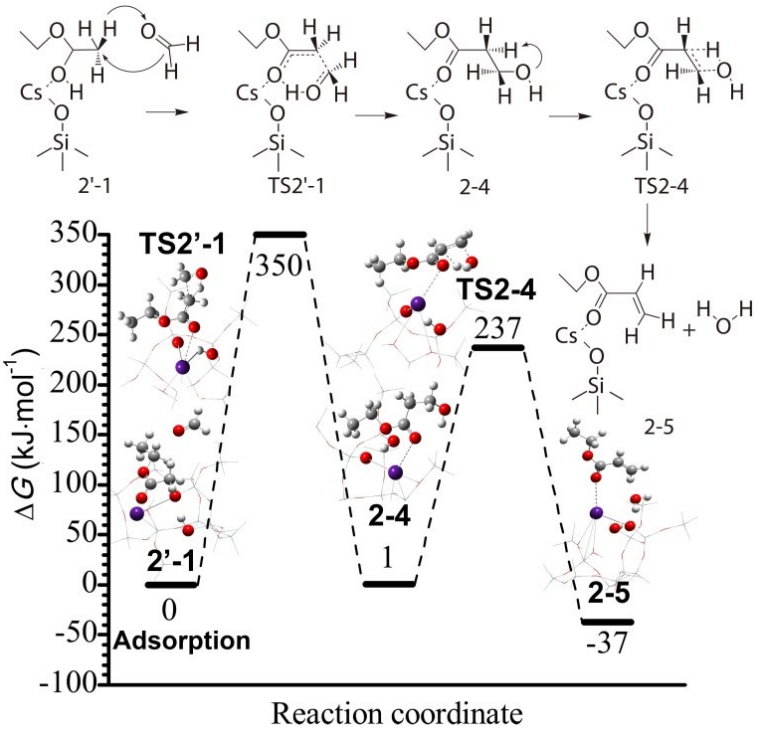

Fig. S10. The scheme and the total energy diagram for the pathway of aldol condensation between Ea and FA through the straight condensation on the active surface model of Cs/SBA-15.

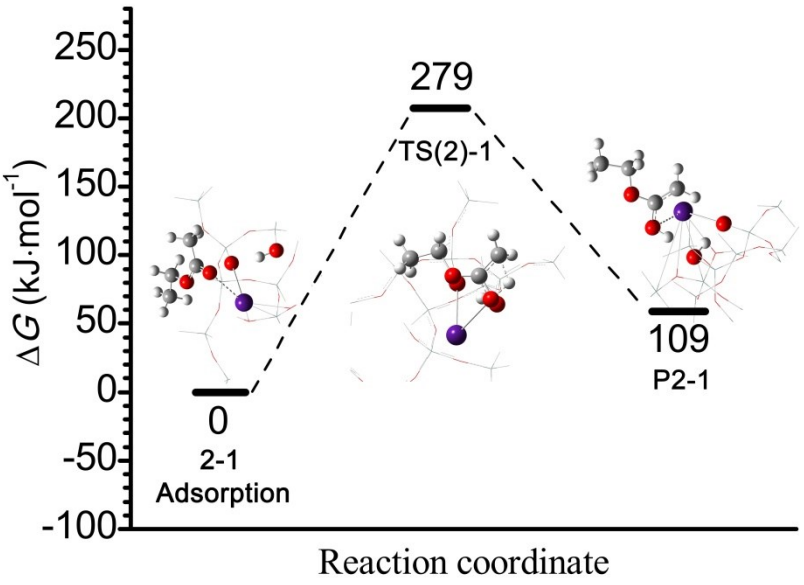

Fig. S11. Change of Gibbs free energy in enol structure formation without silicon hydroxyl on the active surface model of Cs/SBA-15.

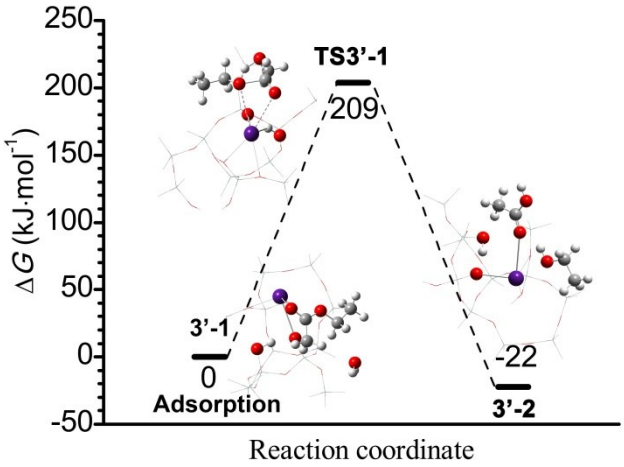

Fig. S12. Change of Gibbs free energy for the hydrolysis pathway of Ea on the active surface model of Cs/SBA-15.

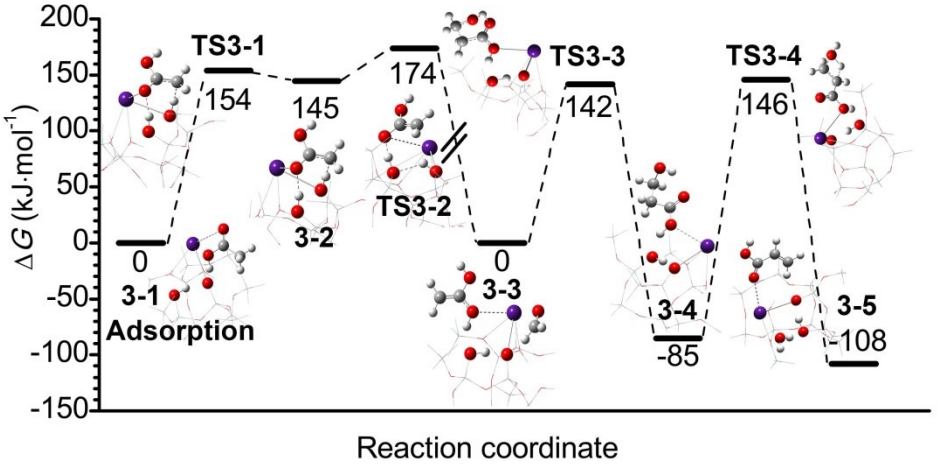

Fig. S13. Change of Gibbs free energy for the aldol condensation pathway of Aa and FA on the active surface model of Cs/SBA-15.

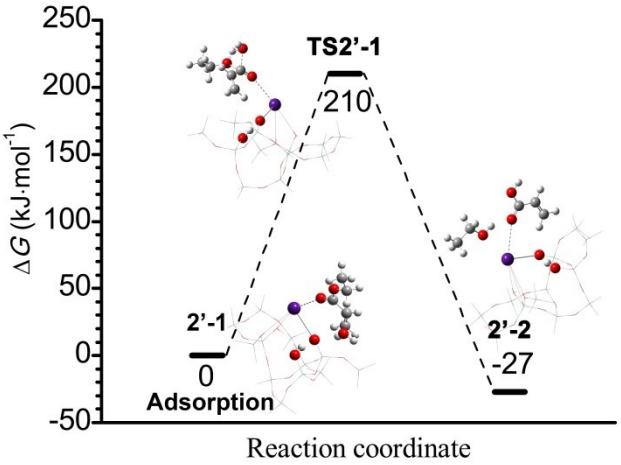

Fig. S14. Change of Gibbs free energy for the hydrolysis pathway of EA on the active surface model of Cs/SBA-15.

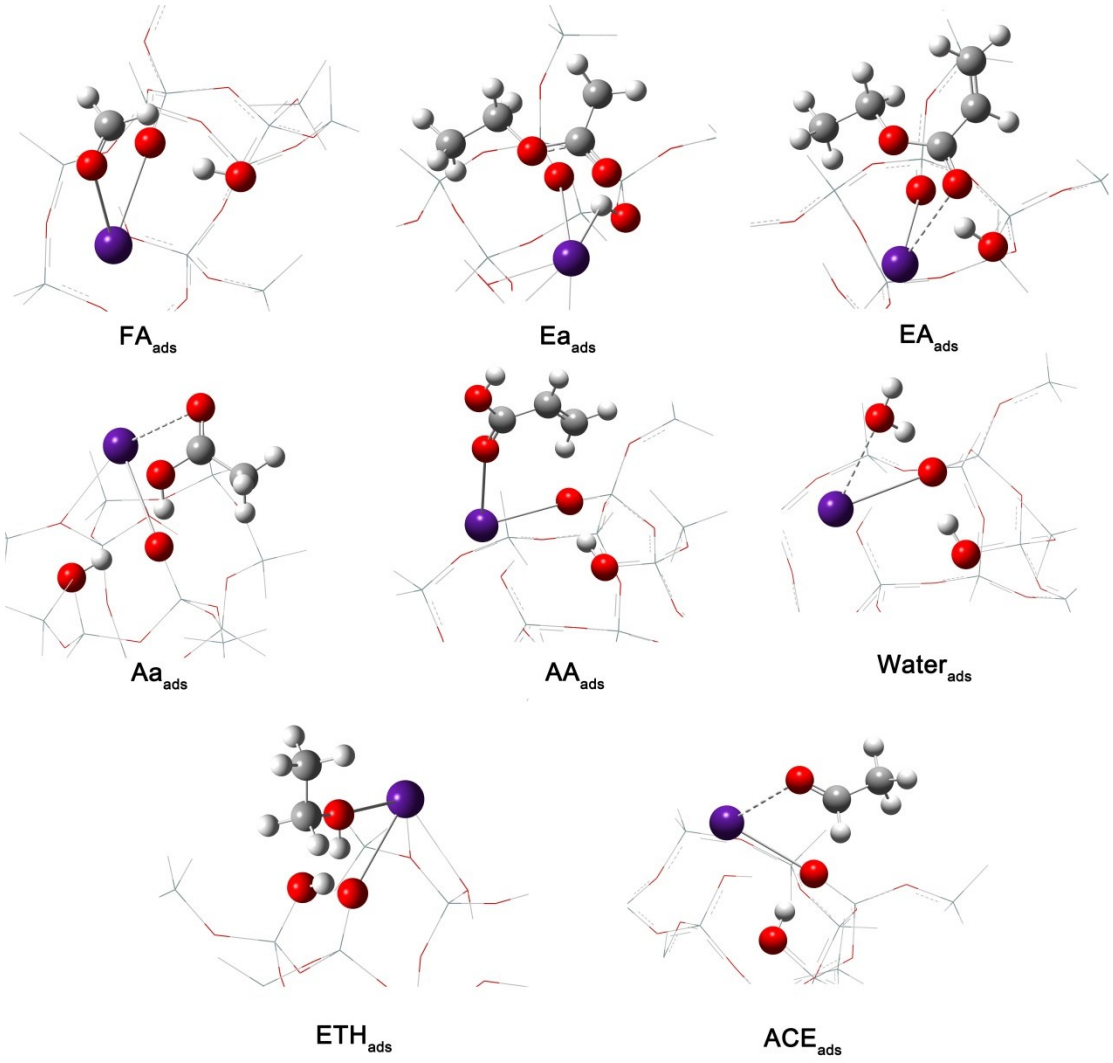

Fig. S15. Conformations of the different substrates in adsorption state.

Table S1 Catalytic performance of xCs/SBA-15 on aldol condensation of ethyl acetate and FA in stability tests.[a]

Loading (wt. %)	Time (h)	TOF (h^{-1})						Y(S) (%)		Molar ratio[d]	B_m (%)
		EA+AA	ACE	Ma	ACR	SUM_{ACE} [b]	PA	EA+AA	Others[c]		
3	2+3	103.3	16.4	2.0	2.8	21.2	8.3	61(88)	8(12)	7.7	98
	4+5	101.9	16.5	1.9	2.7	21.1	8.1	60(89)	7(11)	8.2	98
	6+7	98.9	16.3	1.7	2.3	20.3	7.7	58(89)	7(11)	8.8	96
5	2+3	65.3	10.6	3.1	3.8	17.5	4.5	63(85)	11(15)	3.2	97
	4+5	61.2	12.1	2.6	2.8	17.5	4.3	59(86)	9(14)	4.1	96
	6+7	57.9	12.7	2.2	2.8	17.7	5.3	56(85)	10(15)	5.0	94
8	2+3	39.9	4.5	1.3	1.8	7.6	2.6	60(87)	9(13)	3.0	94
	4+5	36.4	4.8	1.1	1.6	7.5	2.6	55(87)	8(13)	4.0	93
	6+7	33.6	5.5	1.1	1.5	8.1	2.8	50(86)	8(14)	4.6	92
10	2+3	31.3	3.7	1.2	1.3	6.2	2.1	58(87)	8(13)	2.6	92
	4+5	28.7	3.9	1.1	1.2	6.1	2.4	53(86)	8(14)	3.1	91
	6+7	26.5	4.2	0.9	1.1	6.2	1.8	49(87)	7(13)	3.7	88

EA, AA, ACE, Ma, ACR, and PA represent ethyl acrylate, acrylic acid, acetaldehyde, methyl acetate, acrolein and propionic acid, respectively.

[a] *T*rxn = 663 K, SV = 20 $mL \cdot h^{-1} \cdot g_{cat}^{-1}$, *n*(formaldehyde): *n*(ethyl acetate): *n*(ethanol) = 1: 2.5: 4

[b] Summed TOF for ACE, Ma and ACR.

[c] Summed yield (selectivity) for Ma, ACR and PA.

[d] Molar ratio of AA/EA in product.

Table S2 The change of Gibbs free energies of the substitution for Cs-O(x)-SBA-15.

Model	$\Delta G_{\text{Cs-O(x)-SBA-15}}$ (kJ/mol)
Cs-O(1)-SBA-15	-386.10
Cs-O(2)-SBA-15	-432.67
Cs-O(3)-SBA-15	-445.08

Table S3 The distances between atoms of conformations in the ethanol dehydrogenation process.

Models	Distance between two atoms (Å)					
	C_{α}-O_{ETH}	C_{α}-H_{α}	O_{ETH}-H_{ETH}	$H_{O(2)}$-O_{ETH}	$H_{O(2)}$-$O_{(2)}$	H_{ETH}-O_{base}
1-1	1.42	1.10	1.00	-	-	-
Trans1-1	1.42	1.10	1.03	1.90	0.98	1.51
TS1-1	1.25	1.72	2.61	1.80	0.99	1.28
1-2	-	-	-	-	-	-

Table S4 The structural parameters for the optimized geometries of the molecules during the activation process to form enol structure from ethyl acetate involving silicon hydroxyl.

Models	Dihedral angle(°)		Distance between two atoms (Å)			
	$H_{O(2)}$-$O_{(2)}$-Cs-O_{base}	$O_{(2)}$-O_{base}-Cs-H_{α}	H_{α}-C_{α}	H_{α}-O_{base}	$H_{O(2)}$-$O_{(2)}$	$H_{O(2)}$-$O_{(c)}$
2-1	-	-	-	-	-	-
Trans2-1	13	101	1.10	2.04	1.00	2.42
TS 2-1	85	94	1.55	1.13	1.00	1.74
2-2	86	94	1.73	1.06	1.00	1.68
TS2-2	126	36	2.50	0.98	1.07	1.41
P 2-1	126	~0	3.42	1.48	1.79	0.99